NIH Public Access
Author Manuscript
Nat Med. Author manuscript; available in PMC 2010 March 24.

Published in final edited form as:
Nat Med. 2009 April ; 15(4): 377–379. doi:10.1038/nm.1940.

Amyloid precursor protein secretases as therapeutic targets for traumatic brain injury

David J Loane[1], **Ana Pocivavsek**[1], **Charbel E-H Moussa**[1], **Rachel Thompson**[1], **Yasuji Matsuoka**[2], **Alan I Faden**[1], **G William Rebeck**[1], and **Mark P Burns**[1]

[1] Department of Neuroscience, Georgetown University Medical Center, Washington, DC, USA

[2] Department of Neurology, Georgetown University Medical Center, Washington, DC, USA

Abstract

Amyloid-β (Aβ) peptides, found in Alzheimer's disease brain, accumulate rapidly after traumatic brain injury (TBI) in both humans and animals. Here we show that blocking either β- or γ-secretase, enzymes required for production of Aβ from amyloid precursor protein (APP), can ameliorate motor and cognitive deficits and reduce cell loss after experimental TBI in mice. Thus, APP secretases are promising targets for treatment of TBI.

TBI is the leading cause of mortality and disability among young individuals in developed countries, and globally the incidence of TBI is rising sharply[1]. TBI is a disease process, with an initial injury that induces biochemical and cellular changes that contribute to continuing neuronal damage and death over time. This continuing damage is known as secondary injury, and multiple apoptotic and inflammatory pathways are activated as part of this process (for reviews, see refs. [2,3]). TBI is a major risk factor for the development of Alzheimer's disease[4,5], and post-mortem studies show that 30% of TBI fatalities have Aβ deposits[6,7]. Remarkably, these deposits may occur less than 1 d after injury[8]. Not only does Aβ accumulate after TBI[9,10], but also do the necessary APP enzymes responsible for Aβ production: β-APP–cleaving enzyme-1 (BACE1) and presenilin-1, a γ-secretase complex protein[11–14]. Although the role of the APP secretases in secondary injury is unknown, multiple lines of evidence show that Aβ can cause cell death, activate inflammatory pathways[15–18] and prime proapoptotic pathways for activation by other insults[19]. The APP secretases may also be directly involved in secondary injury, as over-expressed *BACE1* alone has been shown to cause neuronal cell loss in the absence of Aβ accumulation[20]. These facts make the APP secretases a potential therapeutic target for TBI.

In our initial experiments, we characterized the TBI-induced protein changes in a nontransgenic mouse. We performed TBI by controlled cortical impact (CCI) of the left parietal cortex. This model induces both necrotic and apoptotic cell death, causing brain lesion and the development of behavioral deficits[21]. It has recently been reported that interstitial fluid Aβ concentrations correlate with neurological function in the injured human brain, with Aβ accumulating as neurological function improved in the days after trauma[22]. Exposure to experimental TBI resulted in accumulation of endogenous mouse $A\beta_{x\text{-}40}$ peptide in the ipsilateral cortex within 1 d (Fig. 1a). Aβ levels increased by almost 120% at 3 d after injury before normalizing by 7 d (Fig. 1a). The accumulation of Aβ corresponded with increased protein amounts of APP,

Correspondence should be addressed to M.P.B. (mpb37@georgetown.edu).

Note: Supplementary information is available on the Nature Medicine website.

Reprints and permissions information is available online at http://npg.nature.com/reprintsandpermissions/

NIH-PA Author Manuscript
NIH-PA Author Manuscript
NIH-PA Author Manuscript

NIH-PA Author Manuscript

NIH-PA Author Manuscript

NIH-PA Author Manuscript

Bace1 and presenilin-1 (Fig. 1b), as has been previously reported in other animal models and humans[9–14]. Soluble APP-α, which is purported to be neuroprotective[23], was also increased after injury. Functionally, this model of TBI causes deficits in fine motor coordination (beam walk test, Supplementary Fig. 1a online) in the absence of gross motor deficits (open-field test, Supplementary Fig. 1b). Injured mice also have hippocampal deficits, with reduced spatial learning in a Morris water maze test (escape latency and probe trial, Supplementary Fig. 1c,d). TBI did not cause any alterations in the ability of the mice to find a visual platform, nor did it affect the swim speed of the mice (Supplementary Fig. 1e,f).

To test the effect of β-secretase on TBI outcome, we used the *Bace1*$^{-/-}$ mouse. Bace1 is the initial rate-limiting enzyme for Aβ production. *Bace1*$^{-/-}$ mice are unable to produce any species of Aβ[24], and we confirmed the absence of $A\beta_{x\text{-}40}$ in brain homogenates by ELISA (0.1 ± 0.09 fmol per mg protein). We performed CCI surgery, and we used the beam walk test to detect fine motor coordination aberrations[21]. This test examines the number of errors (foot faults) made by the right hind limb over 50 steps. We trained the mice on the test before injury, and we repeated this test on 1 d, 3 d, 7 d, 14 d and 21 d after TBI. Injured *Bace1*$^{-/-}$ mice made significantly fewer foot faults at multiple time points, with a 38% final improvement over injured *Bace1*$^{+/+}$ mice (Fig. 1c, $P < 0.001$).

We used a Morris water maze paradigm to assess spatial learning by training mice to locate a hidden, submerged platform using extramaze visual information[21]. The test was conducted at 15–18 d after injury, and each mouse was tested for four trials per day for four consecutive days. Uninjured *Bace1*$^{+/+}$ mice were used as a behavioral control. Injured *Bace1*$^{+/+}$ mice had significant learning impairments on all 4 d of testing compared to uninjured *Bace1*$^{+/+}$ mice ($P < 0.01$). Injured *Bace1*$^{-/-}$ mice, however, improved rapidly, and on the final day of testing were indistinguishable from uninjured mice (Fig. 1d, $P < 0.01$ for injured *Bace1*$^{-/-}$ versus injured *Bace1*$^{+/+}$). All groups had similar escape latencies when presented with a visual platform probe test (uninjured *Bace1*$^{+/+}$, 23.4 ± 6.3 s; injured *Bace1*$^{+/+}$, 21.1 ± 7.8 s; injured *Bace1*$^{-/-}$, 21.2 ± 4.9 s).

Five mice in each TBI group were randomly chosen for T2-weighted magnetic resonance imaging (MRI) analysis at 21 d after trauma. MRI assessment of damage in injured *Bace1*$^{+/+}$ mice showed that the lesion was extensive, spreading from the cortex through the hippocampus and connecting to the lateral ventricles. However, injured *Bace1*$^{-/-}$ mice showed considerable sparing of brain tissue, particularly of the ipsilateral hippocampus (Fig. 1e). This was confirmed in fixed brain tissue sections (Fig. 1f). Quantitative analyses showed that injured *Bace1*$^{+/+}$ mice lost 65.4% ± 6.8% of hippocampal tissue, compared to only 9.0% ± 5.3% for injured *Bace1*$^{-/-}$ mice (Fig. 1g, $P < 0.01$). Total lesion volume was reduced by 30% in injured *Bace1*$^{-/-}$ mice (Fig. 1h, $P < 0.05$).

The other secretase involved in amyloidogenic processing of APP is γ-secretase, and we used the pharmacological inhibitor *N*-[*N*-(3, 5-difluorophenacetyl-L-alanyl)]-S-phenylglycine *t*-butyl ester (DAPT) to block enzyme activity. Previous work has shown that familial presenilin-1 mutations known to cause Alzheimer's disease increase Aβ levels by 30%[25], suggesting that this level of inhibition would be sufficient to prevent a disease state. We administered DAPT orally at 30 mg per kg body weight, a dose that has previously been shown to reduce Aβ levels *in vivo*[26]. Each mouse received the initial dose 15 min after CCI or sham surgery and then twice daily for 21 d. We implemented this dosing regime because Aβ levels are known to drop after γ-secretase inhibition before recovering over several hours[27,28]. To confirm γ-secretase inhibition in DAPT-treated mice, we measured Aβ concentrations. Three hours after the final drug administration, Aβ levels were reduced by 25% (13.76 ± 0.8 fmol per mg protein (vehicle-treated TBI mice) versus 10.42 ± 0.4 fmol per mg protein (DAPT-

NIH-PA Author Manuscript

NIH-PA Author Manuscript

NIH-PA Author Manuscript

treated TBI mice); $P < 0.01$), and APP carboxy-terminal fragments accumulated (Supplementary Fig. 2b online).

We conducted the first beam walk test on the day after CCI. Vehicle-treated TBI mice made 50 ± 0 foot faults and improved to 43 ± 2 foot faults on the final day of testing (Fig. 2a). DAPT-treated TBI mice had a foot fault rate of 48 ± 1 on the day after surgery; however, by 21 d after injury, they averaged 25 ± 5 foot faults, a significant improvement of 42% over vehicle-treated TBI mice (Fig. 2a, $P < 0.001$). We tested spatial learning with the Morris water maze. Vehicle-treated TBI mice had significant learning impairments on all 4 d of the test, whereas the behavior of DAPT-treated TBI mice was indistinguishable from sham-injured mice (Fig. 2b). All mice had similar swim speeds in the maze (Fig. 2c), and similar escape latencies when presented with a visible platform probe (vehicle-treated, sham-operated mice, 15.5 ± 3.1 s; DAPT-treated, sham-operated mice, 13.6 ± 3.4 s; vehicle-treated TBI mice, 15.1 ± 2.6 s; DAPT-treated TBI mice, 17.5 ± 3.7 s).

MRI revealed that DAPT treatment substantially reduced lesion size in injured mice (Fig. 2d). The representative MRI images show a vehicle-treated TBI mouse with the brain lesion visible through 4 mm (8 mm × 0.5 mm longitudinal sections) of tissue, whereas DAPT treatment results in damage through only 1.5 mm (3 mm × 0.5 mm sections; Fig. 2d). Histological assessment showed that DAPT treatment spared large areas of cortex and subcortical white matter tracts, notably the corpus callosum (Fig. 2e), and decreased lesion volume by > 70% ($P < 0.01$, Fig. 2f). The damage to the hippocampus was not as extensive as that seen in the *Bace1* study; however, cell loss in the CA1 region of mice after TBI was clearly visible (Fig. 2g). This allowed quantification of cell loss in the hippocampus (Fig. 2h). We stained neurons with NeuN, a neuronal marker, and performed an unbiased stereology count. TBI caused a 34% decrease in NeuN-positive cells in the CA1 region of the ipsilateral hippocampus ($P < 0.05$). DAPT treatment significantly attenuated this cell loss, resulting in only a 10% reduction in CA1 neurons ($P < 0.05$ versus vehicle-treated TBI mice). Thus, DAPT treatment decreased cell death in hippocampal neurons, reduced cortical cell loss and reduced white matter damage in the corpus callosum. These findings are supported by data from a mouse model of stroke, in which DAPT treatment reduced infarct area and improved neurological function after ischemia and reperfusion[29].

The temporal dissociation between the peak of APP secretase protein abundance (day 3) and the learning improvements (day 18) suggest that the APP secretases have a detrimental role in the initiation of secondary injury, rather than continually producing a toxic factor. By decreasing secretase activity during this crucial period, the ongoing damage of secondary injury can be blocked. Further experiments, such as Aβ rescue in *Bace1*-knockout mice, would definitively test the role of Aβ after TBI; however, our data demonstrate that the APP secretases are key mediators of tissue loss after injury. We have shown that knockout of the *Bace1* gene decreases cell loss and behavioral deficits in a classically used TBI mouse model. Similarly, pharmacological inhibition of γ-secretase activity reduces post-traumatic tissue loss and improves motor and cognitive recovery. Notably, the γ-secretase inhibitor was administered after trauma, modeling a clinically relevant situation. Together, these studies suggest that modulation of APP secretases may provide new therapeutic targets for the treatment of TBI.

Supplementary Material

Refer to Web version on PubMed Central for supplementary material.

Acknowledgments

We would like to thank A. Pajoohesh-Ganji and P. Washington for technical assistance; S. Fricke and O. Rodriguez of the Small Animal Imaging Laboratory at Georgetown University; and P. Mathews (Nathan S. Kline Institute) for

NIH-PA Author Manuscript

NIH-PA Author Manuscript

NIH-PA Author Manuscript

antibody C1/6.1. This work was funded by grant R03NS57635 (M.P.B.) and a pilot award from the National Capital Area Rehabilitation Research Network R24HD050845 (M.P.B.), both from the US National Institutes of Health, and by the Klingel Family Foundation (M.P.B.).

References

1. Maas AI, Stocchetti N, Bullock R. Lancet Neurol 2008;7:728–741. [PubMed: 18635021]
2. Lenzlinger PM, Morganti-Kossmann MC, Laurer HL, McIntosh TK. Mol Neurobiol 2001;24:169–181. [PubMed: 11831551]
3. Zhang X, Chen Y, Jenkins LW, Kochanek PM, Clark RS. Crit Care 2005;9:66–75. [PubMed: 15693986]
4. Mayeux R, et al. Ann Neurol 1993;33:494–501. [PubMed: 8498827]
5. van Duijn CM, et al. Am J Epidemiol 1992;135:775–782. [PubMed: 1595677]
6. Roberts GW, Gentleman SM, Lynch A, Graham DI. Lancet 1991;338:1422–1423. [PubMed: 1683421]
7. Roberts GW, et al. J Neurol Neurosurg Psychiatry 1994;57:419–425. [PubMed: 8163989]
8. Ikonomovic MD, et al. Exp Neurol 2004;190:192–203. [PubMed: 15473992]
9. Chen XH, et al. Am J Pathol 2004;165:357–371. [PubMed: 15277212]
10. Iwata A, Chen XH, McIntosh TK, Browne KD, Smith DH. J Neuropathol Exp Neurol 2002;61:1056–1068. [PubMed: 12484568]
11. Blasko I, et al. J Neural Transm 2004;111:523–536. [PubMed: 15057522]
12. Cribbs DH, Chen LS, Cotman CW, LaFerla FM. Neuroreport 1996;7:1773–1776. [PubMed: 8905662]
13. Nadler Y, et al. Glia 2008;56:552–567. [PubMed: 18240300]
14. Uryu K, et al. Exp Neurol 2007;208:185–192. [PubMed: 17826768]
15. Matsuoka Y, et al. Am J Pathol 2001;158:1345–1354. [PubMed: 11290552]
16. Mattson MP, et al. J Neurosci 1992;12:376–389. [PubMed: 1346802]
17. Wyss-Coray T, Mucke L. Neuron 2002;35:419–432. [PubMed: 12165466]
18. Yankner BA, et al. Science 1989;245:417–420. [PubMed: 2474201]
19. Esposito L, Gan L, Yu GQ, Essrich C, Mucke L. J Neurochem 2004;91:1260–1274. [PubMed: 15584903]
20. Rockenstein E, et al. J Biol Chem 2005;280:32957–32967. [PubMed: 16027115]
21. Fox GB, Fan L, Levasseur RA, Faden AI. J Neurotrauma 1998;15:599–614. [PubMed: 9726259]
22. Brody DL, et al. Science 2008;321:1221–1224. [PubMed: 18755980]
23. Thornton E, Vink R, Blumbergs PC, Van Den HC. Brain Res 2006;1094:38–46. [PubMed: 16697978]
24. Cai H, et al. Nat Neurosci 2001;4:233–234. [PubMed: 11224536]
25. Duff K, et al. Nature 1996;383:710–713. [PubMed: 8878479]
26. Dovey HF, et al. J Neurochem 2001;76:173–181. [PubMed: 11145990]
27. Abramowski D, et al. J Pharmacol Exp Ther 2008;327:411–424. [PubMed: 18687920]
28. El Mouedden M, Vandermeeren M, Meert T, Mercken M. Curr Pharm Des 2006;12:671–676. [PubMed: 16472156]
29. Arumugam TV, et al. Nat Med 2006;12:621–623. [PubMed: 16680150]

NIH-PA Author Manuscript

NIH-PA Author Manuscript

NIH-PA Author Manuscript

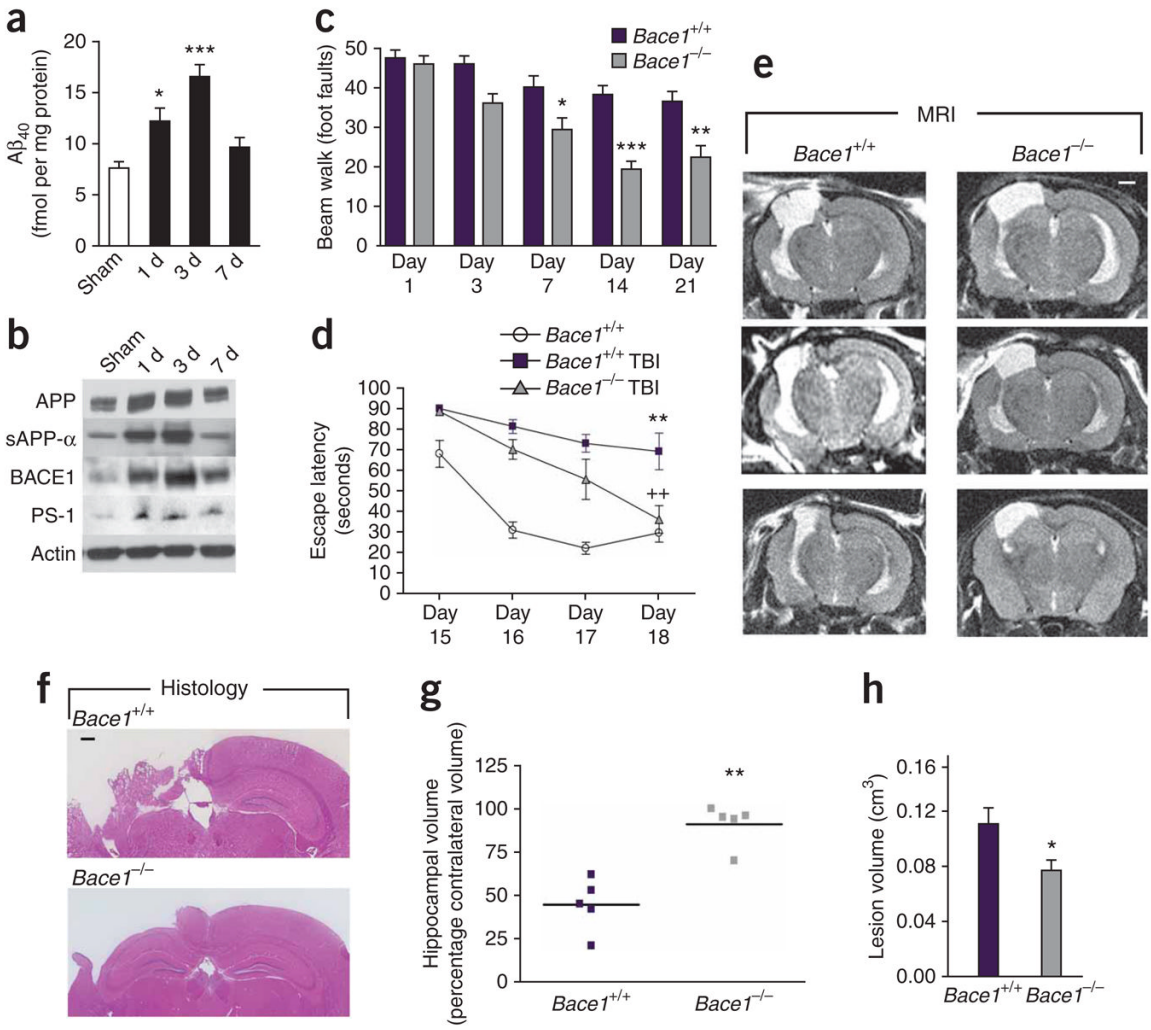

Figure 1.

Bace1 ablation protects against TBI-induced cell loss and behavioral deficits *in vivo*. (**a**) Quantification of $A\beta_{x\text{-}40}$ in the ipsilateral cortex 1 d, 3 d and 7 d after controlled cortical contusion injury, as outlined in the Supplementary Methods online. **P* < 0.05 and ****P* < 0.001 versus sham control by analysis of variance (ANOVA), Neuman-Keuls *post-hoc* test. Data are means ± s.e.m.; *n* = 4. (**b**) Western blot analysis of the amyloid-related proteins APP, sAPP-α, BACE1 and presenilin-1 (PS-1) after TBI in nontransgenic mice. Blots are representative of three separate experiments. (**c**) Fine motor coordination test on a beam walk apparatus. Deficits in coordination are recorded as foot faults. **P* < 0.05, ***P* < 0.01 and ****P* < 0.001 by ANOVA, Newman-Keuls *post-hoc* test. Data are means ± s.e.m.; *n* = 8. (**d**) Spatial learning in a Morris water maze. Each trial is the average of four individual tests, and four trials were performed with the escape latency to the platform being recorded. ***P* < 0.01 versus uninjured *Bace1*$^{+/+}$ and ++*P* < 0.01 versus injured *Bace1*$^{+/+}$ by ANOVA, Newman-Keuls *post-hoc* test. Data are means ± s.e.m. *n* = 5 for *Bace1*$^{+/+}$ and *n* = 8 for TBI groups. (**e**) T2-weighted MRI images from TBI mice 21 d after injury. Representative images from three different mice in each group. Lesions of the left hemisphere appear white on the images (scale bar, 1mm). (**f**) Representative images of H&E-stained sections, highlighting hippocampal sparing in injured *Bace1*$^{-/-}$ mice. Scale bar, 500 μm. (**g**) Hippocampal volume, as assessed by comparing tissue remaining in the ipsilateral side with the contralateral hippocampus. ***P* <

NIH-PA Author Manuscript

NIH-PA Author Manuscript

NIH-PA Author Manuscript

0.01 by Mann-Whitney *U* test, $n = 5$. (**h**) Lesion volume 21 d after injury. $^*P < 0.05$ by Student's t test; data are means ± s.e.m., $n = 5$. All procedures were reviewed and approved by the Georgetown University Animal Care and Use Committee.

NIH-PA Author Manuscript
NIH-PA Author Manuscript
NIH-PA Author Manuscript

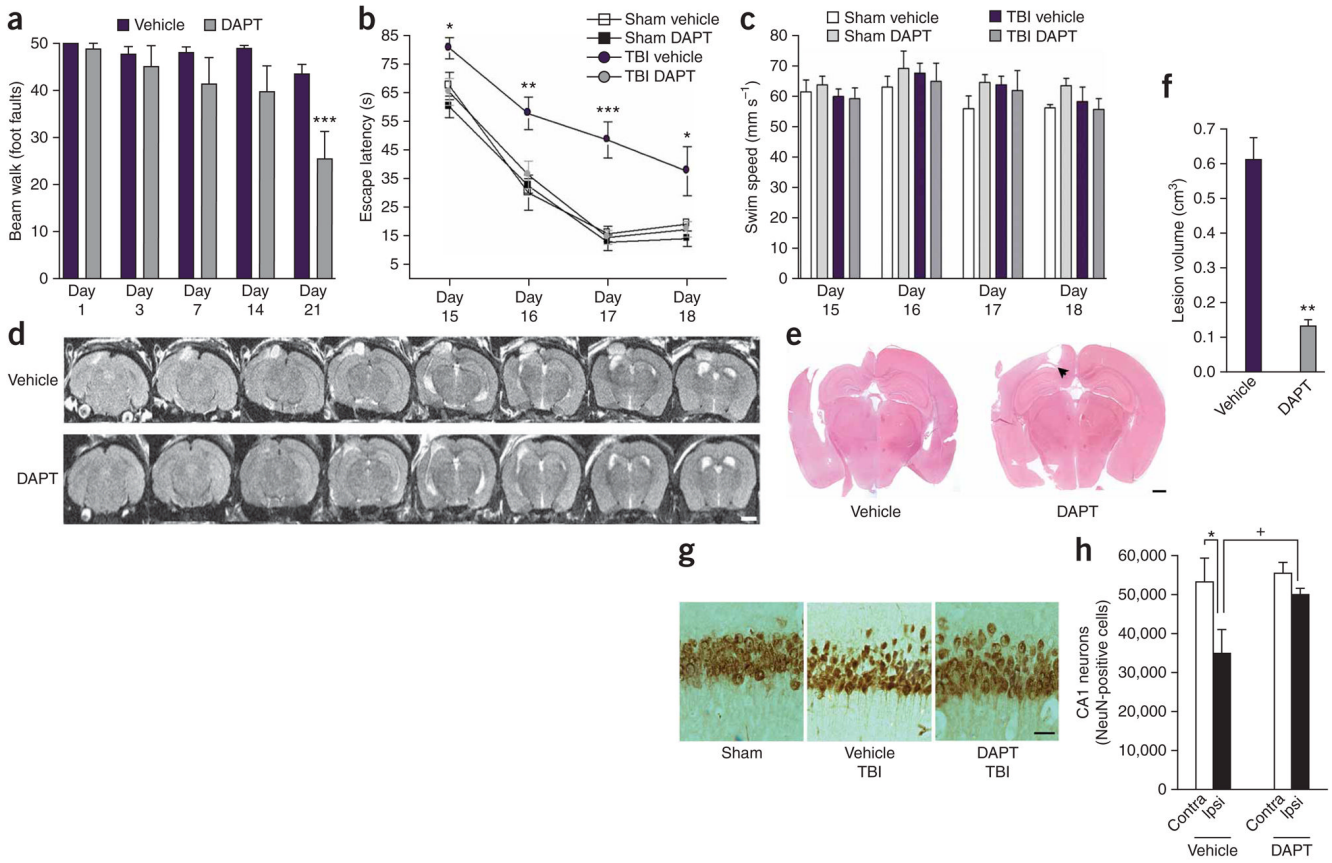

Figure 2.

Chronic γ-secretase inhibition protects against TBI-induced cell loss and behavioral deficits *in vivo*. (**a**) Fine motor coordination test on a beam walk apparatus. Deficits in coordination are recorded as foot faults. ***$P < 0.001$ by ANOVA, Newman-Keuls *post-hoc* test. Data are means ± s.e.m. $n = 11$ for vehicle and $n = 8$ for DAPT. (**b**) Spatial learning in a Morris water maze. *$P < 0.05$, **$P < 0.01$ and ***$P < 0.001$ versus vehicle sham by ANOVA, Newman-Keuls *post-hoc* test. Data are means ± s.e.m. $n = 6$ for sham groups, $n = 11$ for vehicle-treated TBI mice and $n = 8$ for DAPT-treated TBI mice. (**c**) Swim speed measures from the water maze test in **b**. (**d**) Successive T2-weighted MRI slices showing the depth of lesion volume in 21 d CCI-injured mice. The top panels show a vehicle-treated mouse with the lesion clearly visible through eight consecutive 0.5-mm slices (region of hyperintensity in the upper left region of the brain). The bottom panels show the extent of injury in a mouse chronically treated with DAPT. Scale bar, 2 mm; representative images shown, $n = 6$. (**e**) Representative H&E-stained sections showing the extent of tissue sparing in DAPT-treated mice. Subcortical white matter tracts are spared in DAPT treated mice (arrowhead). Scale bar, 750 μm. (**f**) Quantification of lesion volume. **$P < 0.01$ by Student's *t* test. Data are means ± s.e.m. $n = 4$. (**g**) Representative images of NeuN-stained CA1 neurons showing neuronal damage in mice after TBI. Scale bar, 100 μm. (**h**) Stereological cell counts comparing NeuN-positive cells from the ipsilateral (Ipsi) CA1 region of the hippocampus to the contralateral (Contra) CA1 of vehicle and DAPT-treated TBI mice. *$P < 0.05$ and +$P < 0.05$ by ANOVA, Newman-Keuls *post-hoc* test. Data are means ± s.e.m., $n = 3$.